LM-00K041
May 30, 2000

Measurements of Conversion Efficiency for a Flat Plate Thermophotovoltaic System Using a Photonic Cavity Test System

E.J. Brown, C.T. Ballinger, S.R. Burger, G.W. Charache, L.R. Danielson, D.M. DePoy, T.J. Donovan, M. LoCascio

NOTICE

MEASUREMENTS OF CONVERSION EFFICIENCY FOR A FLAT PLATE THERMOPHOTOVOLTAIC SYSTEM USING A PHOTONIC CAVITY TEST SYSTEM

EJ Brown, CT Ballinger, SR Burger, GW Charache, LR Danielson,
DM DePoy, TJ Donovan, M LoCascio
Lockheed Martin Corp. Schenectady, New York

ABSTRACT

The performance of a 1 cm^2 thermophotovoltaic (TPV) module was recently measured in a photonic cavity test system. A conversion efficiency of 11.7% was measured at a radiator temperature of 1076°C and a module temperature of 29.9°C. This experiment achieved the highest direct measurement of efficiency for an integrated TPV system. Efficiency was calculated from the ratio of the peak (load matched) electrical power output and the heat absorption rate. Measurements of these two parameters were made simultaneously to assure the validity of the measured efficiency value.

This test was conducted in a photonic cavity which mimicked a typical flat-plate TPV system. The radiator was a large, flat graphite surface. The module was affixed to the top of a copper pedestal for heat absorption measurements. The heat absorption rate was proportional to the axial temperature gradient in the pedestal under steady-state conditions. The test was run in a vacuum to eliminate conductive and convective heat transfer mechanisms.

The photonic cavity provides the optimal test environment for TPV efficiency measurements because it incorporates all important physical phenomena found in an integrated TPV system: high radiator emissivity and blackbody spectral shape, photon recycling, Lambertian distribution of incident radiation and complex geometric effects. Furthermore, the large aspect ratio between radiating surface area and radiator/module spacing produces a view factor approaching unity with minimal 'photon leakage'.

1. INTRODUCTION

Thermophotovolaics (TPV) is a direct energy conversion concept that has seen renewed interest with the development of III-V semiconductor technology. Recent advances have produced low bandgap (0.50-0.55 eV) quaternary material that is lattice-matched to inexpensive substrates (1,2). These developments enable TPV systems to achieve reasonable efficiency and power density with radiators operating at about 1000°C. At relatively low radiator temperatures, there are many viable options for the heat source and a number of applications become attractive.

In a TPV energy conversion system, a heated surface radiates in the mid-IR region and the radiant energy is directed onto photodiodes which are sensitive in this range. Part of the energy is converted into electric power. Systems are configured in flat plate or cylindrical geometry. Figure 1 is a diagram of a typical flat plate TPV unit.

Because of the close proximity of the radiator to the diode, thermophotovoltaic systems are different from photovoltaic (PV) systems in two important respects. First, the incident energy is isotropic in nature as opposed to the collimated radiation found in PV systems. The performance of optical coatings has an angular dependency and this impacts the design of AR coatings in TPV systems. Secondly, the close proximity of the radiator in a TPV system makes "photon recuperation" possible. As shown in Figure 2, approximately 75% of the photons in a blackbody spectrum will have insufficient energy to create a carrier pair in the diode. Typically, PV systems limit absorption of these below-bandgap photons to keep the diodes cool which improves performance. In a TPV system, these excluded photons can be re-absorbed by the radiator, thus improving the overall conversion efficiency. This technique is often referred to as "spectral control".

The measurements described in this paper were carried out in a photonic cavity which mimics the environment of a typical TPV system. The authors favor this technique because the physical parameters governing TPV systems (black body radiators with high emissivity, photon recuperation, Lambertian incident radiation, complex geometric effects, etc.) are difficult to measure separately. Furthermore, their complex interactions pose a difficult modeling challenge and computed efficiency values are subject to question.

Recently, we measured a thermophotovoltaic module which achieved >10% conversion efficiency for the first time (in a photonic cavity environment). Figure 3 presents the measured efficiency as a function of the radiator temperature. Simultaneous measurements of electric power output (load-matched conditions) and the heat absorption rate were made on a 1 cm^2 module. The module used InGaAsSb diodes with a bandgap of 0.52 eV and an advanced design tandem filter for spectral control. The tandem filter was bonded over the fabricated module using optical epoxy. Heat absorption rates were measured at steady-state conditions using the copper pedestal technique. The experiments were analyzed with both simplified infinite plate calculations and a detailed Monte Carlo model. Calculated efficiencies were ~10% higher than measured results.

2. PHOTONIC CAVITY TEST HARDWARE

A. Experimental Arrangement

The measurements described in this paper were performed in a photonic cavity test (PCT) system. This technique is preferable to other measurement systems because it mocks up a prototypic TPV environment. The basic cavity geometry is shown in Figure 4. There is a large (6 cm x 6 cm) square radiator (graphite) which is heated by boralectric heaters which are located above it. Because the radiator is large (compared to the module) and the module-to-radiator spacing is small (2-3 mm), the cavity test behaves as infinitely large surfaces (i.e. view factor=1.0 and there is minimal "photon leakage"). As a result, the energy arriving at the module has a Lambertian angular distribution.

The TPV module was bonded and heat sunk to the top of the copper pedestal; the heat absorption rate in the module was proportional to the axial temperature gradient in the pedestal under steady-state conditions. The module/pedestal unit was surrounded by a shielding system to guard against stray radiant energy. The tests were carried out under vacuum conditions. Figure 5 shows the module/pedestal unit being loaded into the PCT system.

B. Radiator

The radiator in the PCT system is a monolithic piece of pocographite approximately 3 cm thick with a 6 cm x 6 cm radiating surface. It produced a nearly grey body radiant spectrum which had moderate wavelength and emission angle dependent behavior. At 1750°F it radiated approximately 11 watts/cm^2.

Temperature uniformity is a critical issue in these experiments. While a large temperature gradient presents no difficulties from an operational point of view, it would hurt module performance and it would greatly complicate the ability to correlate measurements with computational analyses. Radiator temperature in the PCT system was measured with four N-type thermocouples; they are placed at various radial locations. The maximum spread among the four thermocouples was 13°F which occurred when the radiator was at its highest average temperature of ~1969°F.

C. Pedestal

The copper pedestal technique was used in these experiments to determine the absorbed heating rate (see Figure 4). The copper pedestal is a rectangular parallelepiped (1 cm x 1 cm x 11 cm) with the bottom terminating in a water-cooled block which serves as a fixed temperature cold reservoir. The axial temperature gradient in the pedestal was measured by three E-type thermocouples which were chosen because of their high sensitivity over low (i.e. about 1000°F) temperature ranges. They are spaced a total of 9.5 cm apart

In principle, the rate of heat absorption could be determined from basic conductive heat transfer principles using the published thermal conductivity for copper and the measured temperature gradient:

$$Q = k * A * dT/dx$$

where Q = heat absorption rate
k = thermal conductivity
A = cross sectional area
dT/dx = temperature gradient

However, to enhance the accuracy of the heat absorption measurements, each pedestal is calibrated individually to account for slight differences in thermocouple spacing, cross sectional area, etc.

The calibration procedure was carried out under vacuum; heat was applied to the top of the pedestal at known rates and the resulting temperature gradient was recorded after the system

came to equilibrium. This approach lumps the thermal conductivity, the cross sectional area and the thermocouple spacing into one composite variable which is assumed to remain unchanged throughout subsequent measurements.

D. Shields

The ability to accurately model the heat absorption rate in the module depends on the exclusion of stray radiant energy from the pedestal. This is accomplished by surrounding the pedestal/module with a collection of gold coated shields (see Figure 6). The sides of the pedestal are protected with a can shield which extends the full length of the pedestal. The inner side of the can is gold coated as well to suppress the small amount of heat that could radiantly transfer between the pedestal and the can due to a slight temperature difference.

A thick cap shield provides most of the protection at the top of the unit. The shielding function is completed by a thin (0.020") disk shield which fits in the cap shield and is small enough to permit fine-scale adjustment.

3. EXPERIMENTAL RESULTS

The radiator was heated from above by two boralectric heaters. Upon reaching a desired radiator temperature, the system was allowed to reach thermal equilibrium and the temperature gradient of the pedestal was recorded to determine the heat absorption rate. The current-voltage (IV) data were then measured quickly to prevent excessive electrical heating of the module (from the curve tracer) which would affect results.

The measured conversion efficiency for this test is presented in Figure 3 as a function of the average radiator temperature. Figure 7 shows the heat absorption rate and Figure 8 shows the load-matched (peak) power output; both quantities are shown as a function of the average radiator temperature.

4. MEASUREMENT UNCERTAINTY

A. Efficiency Results and Confidence Intervals

Efficiency results and 95% confidence intervals (CI) for these tests were calculated using documented measurement results, the pedestal calibration data, and instrumentation manufacturer's information regarding random variabilities of measured data. The uncertainties calculated represent random error only and do not estimate potential sources of systematic error, or bias, inherent in the experimental setup.

Module efficiency (η) is defined as

$$\eta = \frac{P_{max}}{Q_{meas}}, \qquad \text{EQN 1}$$

where P_{max} is the maximum power generated by the module and Q_{meas} is the heat absorption rate of the module. The uncertainty of the efficiency calculation is a function of the uncertainty in Q_{meas} due to the calibration curve fit and the uncertainty in the measurement of P_{max}. From the error propagation equation, this relationship can be expressed as

$$\left(\frac{\sigma_\eta}{\eta}\right)^2 = \left(\frac{\sigma_{Qmeas}}{Q_{meas}}\right)^2 + \left(\frac{\sigma_{P\max}}{P_{\max}}\right)^2. \qquad \text{EQN 2}$$

where σ is standard deviation.

Before error propagation can be performed, information must be obtained regarding the individual measurement uncertainties. For the TPV module efficiency experiment, there are three types of measurements: Temperature (°F), Current (amps), and Voltage (volts). Temperature measurements in the pedestal are used with a heat flux calibration curve to determine the second term in Eqn. 2, above. Variability of the pedestal temperature measurements is accounted for in the determination of the calibration curve fit uncertainty and does not need to be known explicitly. Measurements of the current and voltage in the TPV module and their uncertainties are combined to determine the third term in Eqn. 2. Therefore, estimates of the current and voltage measurement uncertainties must be known explicitly.

Because data are not available which would indicate the random error of the specific instruments used in the experiments, vendor estimates of random error for each instrument type are used instead. Table 1 gives the 95% random error confidence intervals for the current and voltage measurements as well as for the radiator temperature measurements.

B. Q_{meas} Calibration Curve Fit Uncertainties

The pedestal calibration consisted of ten measurements obtained using the TPV module mounted to the top of the pedestal run in reverse bias to generate heat. This calibration was performed after the efficiency measurement using the same TPV module and pedestal arrangement.

The calibration data were fitted to a straight line of the form

$$Q_{fit}(\Delta T)[watts] = b_i[watts/F]\cdot\Delta T + b_o[watts]. \qquad \text{EQN 3}$$

Confidence intervals for this line fit are a function of the standard estimate of error (SEE) of the line fit and the critical value of the students-t distribution for the degrees of freedom (DOF) and the desired CI. The SEE is equal to

$$SEE = \sqrt{\frac{\sum_{i=1}^{n}\left(Q_{meas,i} - Q_{fit,i}\right)^2}{n-2}}, \qquad \text{EQN 4}$$

where n is the number of data points, $Q_{meas,i}$ is the measured heat flux for the ith measurement and $Q_{fit,i}$ is the predicted heat flux based on the line fit and ΔT_i . The DOF is equal to the number of data points

for a given calibration data set minus the number of fit parameters (for this case, 2). For a given value of ΔT, the 95% CI on Q_{fit} is

$$\pm t_{n-2,.025} \cdot SEE \cdot \sqrt{\frac{1}{DOF} + \frac{(\Delta T - \overline{\Delta T_{cal}})^2}{\sum_{i=1}^{n} (\Delta T_i - \overline{\Delta T_{cal}})^2} + 1}, \qquad \text{EQN 5}$$

where $\overline{\Delta T_{cal}}$ is the average of the ΔT_i values in the calibration data set. A statistician recommended and reviewed both the form of the line fit and the method of determining the error associated with the calibration curve fits. Figure 9 shows the calibration data and curve fits with 95% CI.

C. P_{max} Uncertainty

P_{max} is equal to the maximum power produced by the TPV module under illumination by the hot radiator. This value is obtained from current and voltage data obtained from the curve tracer. The expression for P_{max} is

$$P_{max} = I_{max} \cdot V_{max}, \qquad \text{EQN 6}$$

where I_{max} and V_{max} are the current and voltage produced by the TPV at the point of maximum power production. The uncertainty in P_{max} is related to the uncertainties in the measured I_{max} and V_{max} by

$$\left(\frac{\sigma_{P\,max}}{P_{max}}\right)^2 = \left(\frac{\sigma_{Imax}}{I_{max}}\right)^2 + \left(\frac{\sigma_{V\,max}}{V_{max}}\right)^2. \qquad \text{EQN 7}$$

Because the uncertainties of the measured currents and voltages are known from vendor estimates, the uncertainty on P_{max} is easily calculated from EQN 7. Table 2 shows the measured P_{max} values from the seven measurements together with the calculated 95% CI.

D. η Uncertainty

The uncertainty in Q_{meas} depends on the uncertainty of the pedestal combined with the uncertainty in P_{max}. Using EQN 2, the 95% confidence intervals for the measured TPV module efficiencies can be determined. Table 3 shows the measured module efficiencies and their calculated 95% CI; Figure 10 is a plot of the efficiency results and corresponding confidence intervals as a function of the radiator temperature.

5. CONCLUSIONS AND POTENTIAL IMPROVEMENTS

These measurements are the first to achieve double-digit efficiency in a TPV system in a photonic cavity environment. The power density under these conditions was 0.42 W/cm^2. Measured efficiency was below predicted values by ~10%; this discrepancy is not completely understood at this time. However, these comparative results represent an improvement in agreement by about a factor of two over previous in-cavity measurements. The error in calculation of the absorbed heat rate was the largest component of the discrepancy between the measured and calculated module efficiency. Possible future improvements include:

a study of interference effects (i.e. scattering light from the metal grid on the front surface of the TPV diode)

increased radiator emissivity will improve both power density and efficiency. For example, if the radiator emissivity had been increased by 10%, the measured efficiency would have increased by 3% (fractional) and the power density would have increased by 6% (fractional). Furthermore, with an improved tandem filter (increased below-bandgap reflectivity), these sensitivities to radiator emissivity are even greater than those seen for the filter used in these measurements.

improve diode and module characterization capability to accurately measure the series and shunt resistances.

Measurement	Estimated Uncertainties (95% CI)
Temperature (°F)	+/- 0.8% on radiator temperature readings - based on the published Omega standard limits of error for N-type thermocouples (+/- 0.75%) plus an additional readout uncertainty of 0.05% superimposed to account for errors associated with the Fluke Hydra Data Bucket. The 0.05% is a rough estimate based on crosschecks with a readout calibration unit.
Voltage (V) Current (amps)	+/- 1.5% of reading + 0.05*(volts or current/div) – this is based on the published data for the curve tracer (Tektronix 360A).

Table 1: Estimated uncertainties for measured quantities

Average Radiator Temp	Pmax	Pmax 95% CI	Relative 95% CI
F	Watts	Watts	%
1607.0	0.2615	0.0181	6.9%
1696.5	0.3557	0.0213	6.0%
1793.5	0.4709	0.0253	5.4%
1803.1	0.4963	0.0263	5.3%
1908.8	0.6257	0.0313	5.0%
1968.3	0.7459	0.0357	4.8%
1969.0	0.7166	0.0349	4.9%

Table 2: **Pmax and 95% Confidence Intervals based on Vendor Estimates of Instrument Uncertainty**

Radiator and Diode Conditions			Efficiency Results		
Radiator Temp [°F]	Pedestal ΔT [°F]	Module Temp [°F]	η	95% CI η	Relative 95% CI [%]
1607.0	11.9	72.61	9.2%	0.69%	7.6%
1696.5	14.7	77.55	10.1%	0.64%	6.4%
1793.5	18.3	83.95	10.7%	0.61%	5.7%
1803.1	18.9	71.99	10.9%	0.59%	5.4%
1908.8	23.5	93.11	11.1%	0.58%	5.2%
1968.3	26.7	85.83	11.7%	0.57%	4.9%
1969.0	26.7	98.73	11.2%	0.56%	5.0%

Table 3: **Measured TPV Module Efficiencies (η) and 95% Confidence Intervals versus Radiator Temp and Diode Temperature.**

FIGURE 1 - Diagram of a TPV direct energy conversion system with front surface filter providing spectral control

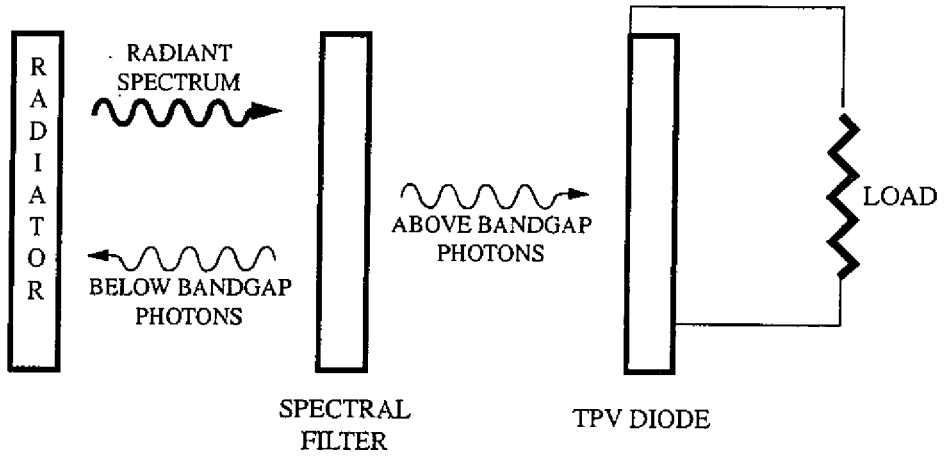

FIGURE 2 - Spectrum from Blackbody Radiator and Convertible portion of a TPV Diode

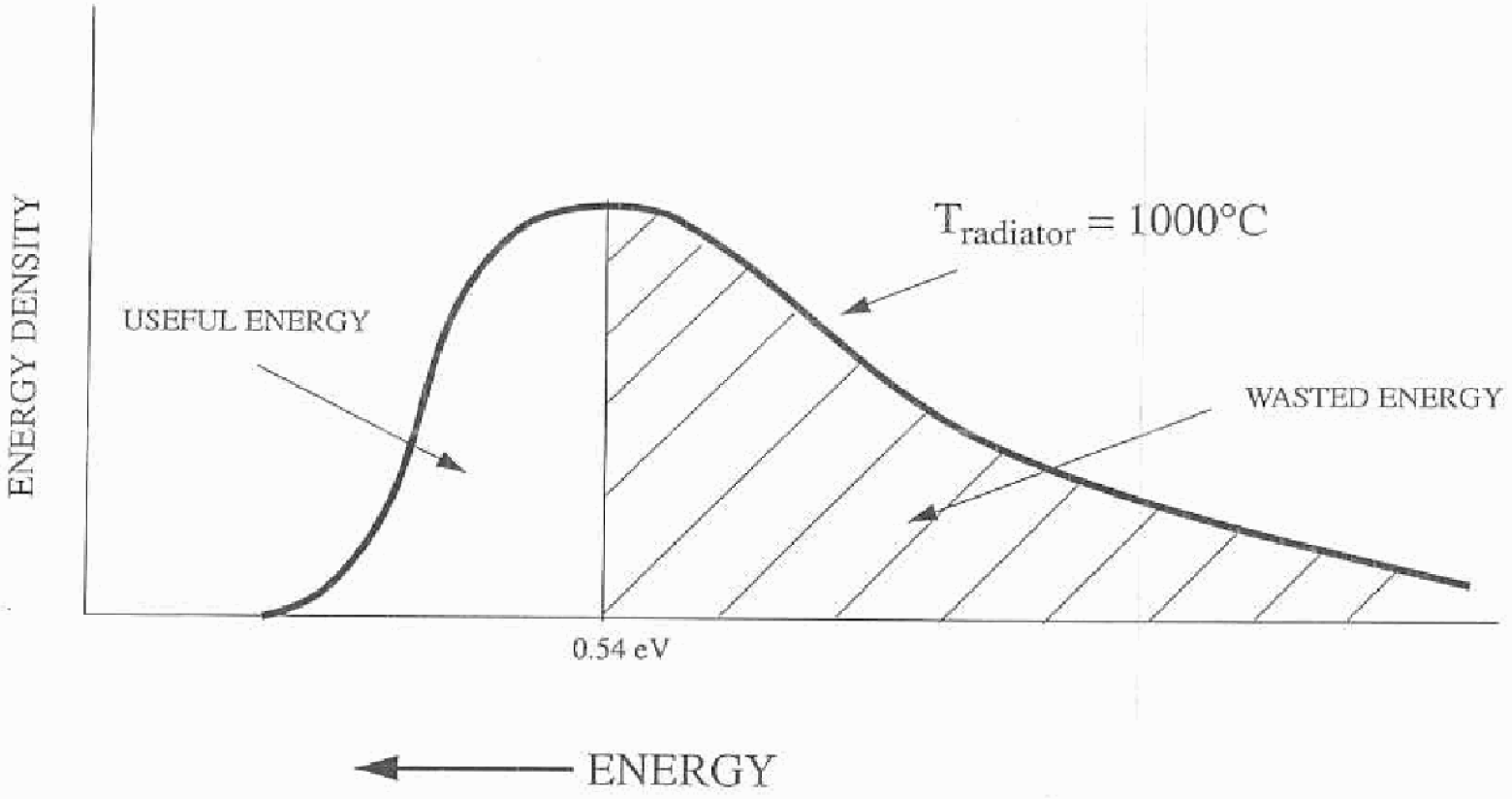

FIGURE 3 - Comparison of Measured to Computed Conversion Efficiency
TPV Module Tested in Photonic Cavity System

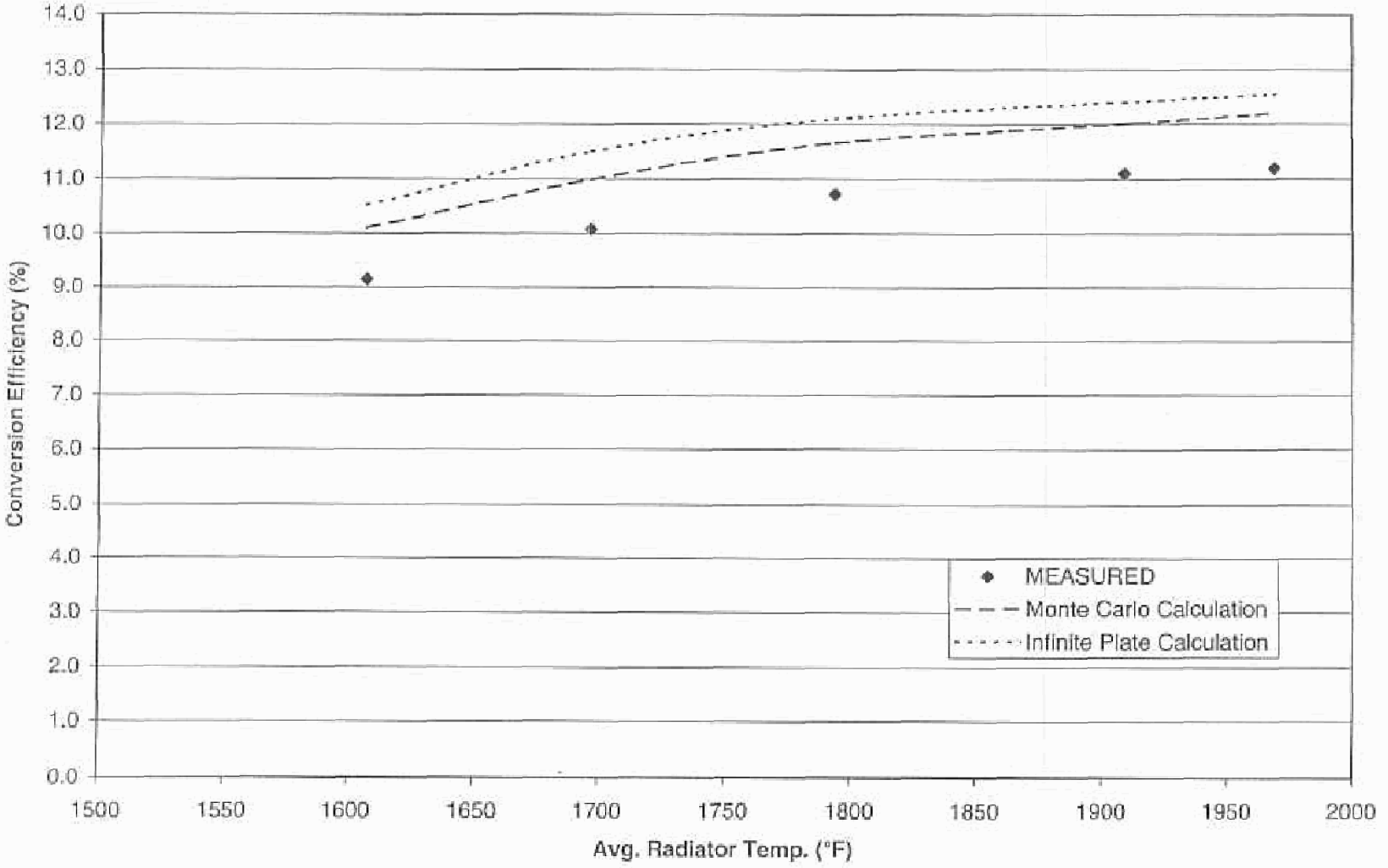

Figure 4 - Photonic Cavity Test System Showing Pedestal, Module, Shields, Radiator and Electric Heaters

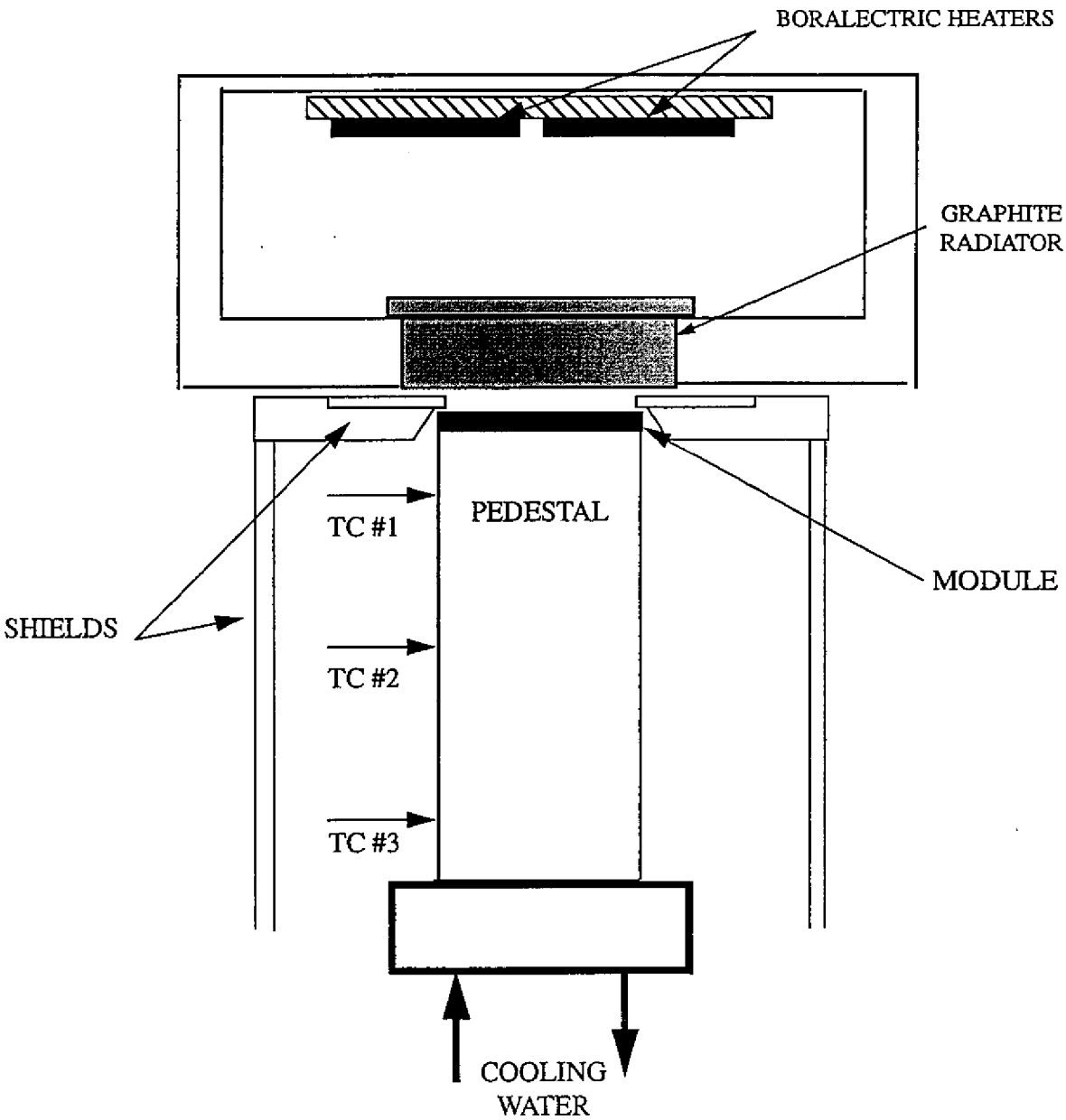

FIGURE 5

Module and Shielding Structure Being Placed into the
Photonic Cavity Test System Prior to Testing

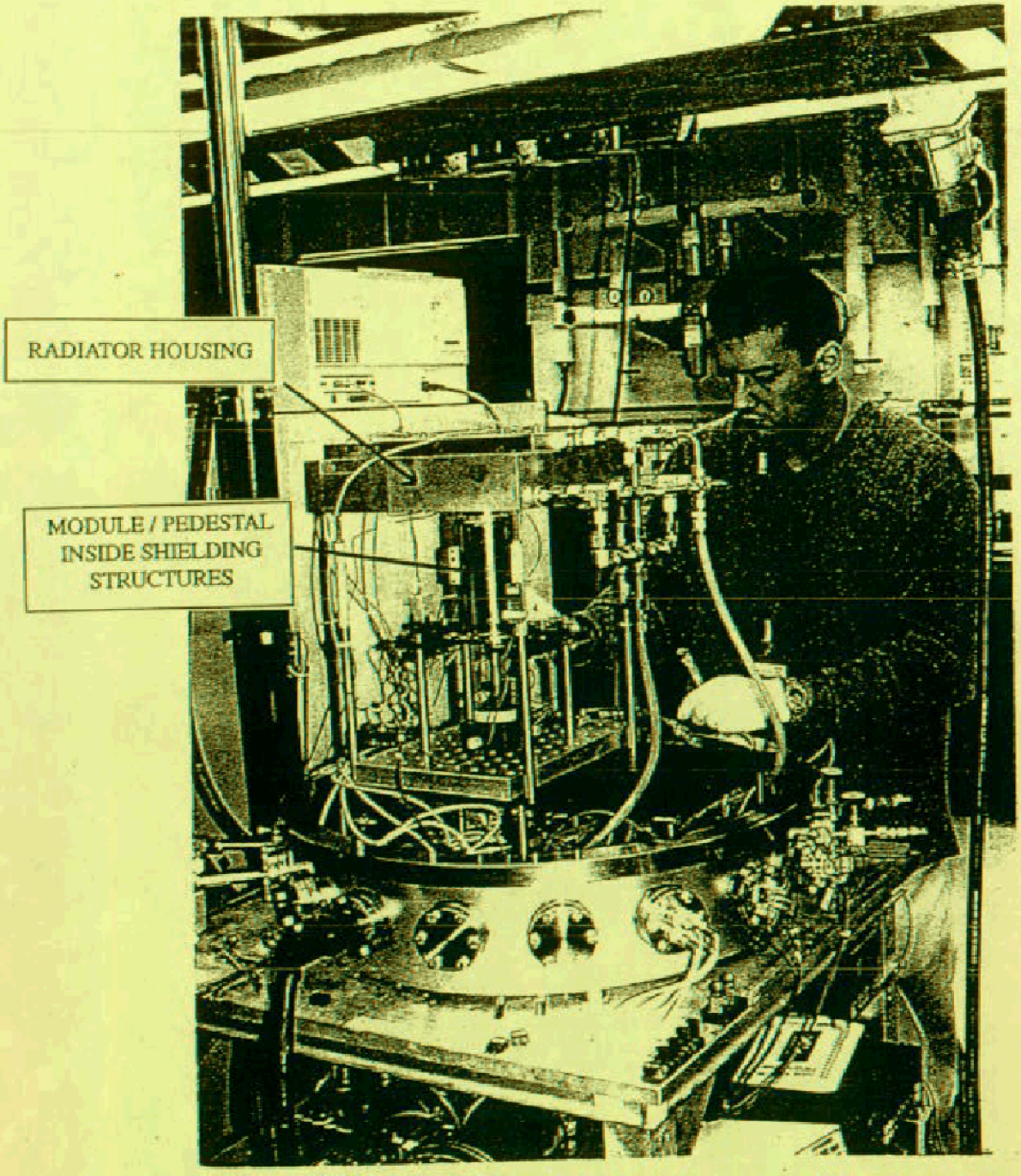

FIGURE 6

Module Beneath Cap and Disk Shields

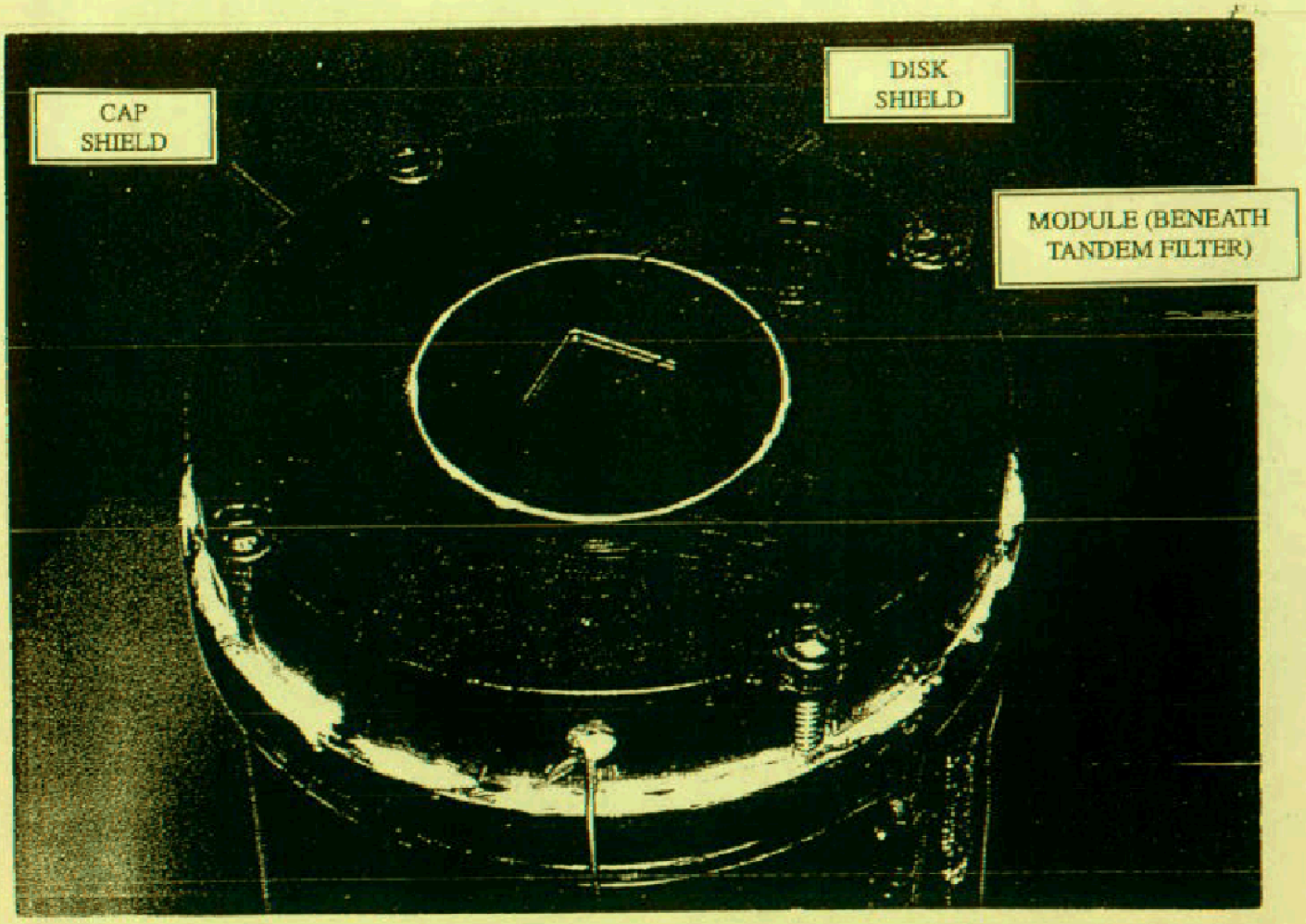

FIGURE 7 - Comparison of Measured to Computed Heat Absorption Rate
TPV Module Tested in Photonic Cavity System

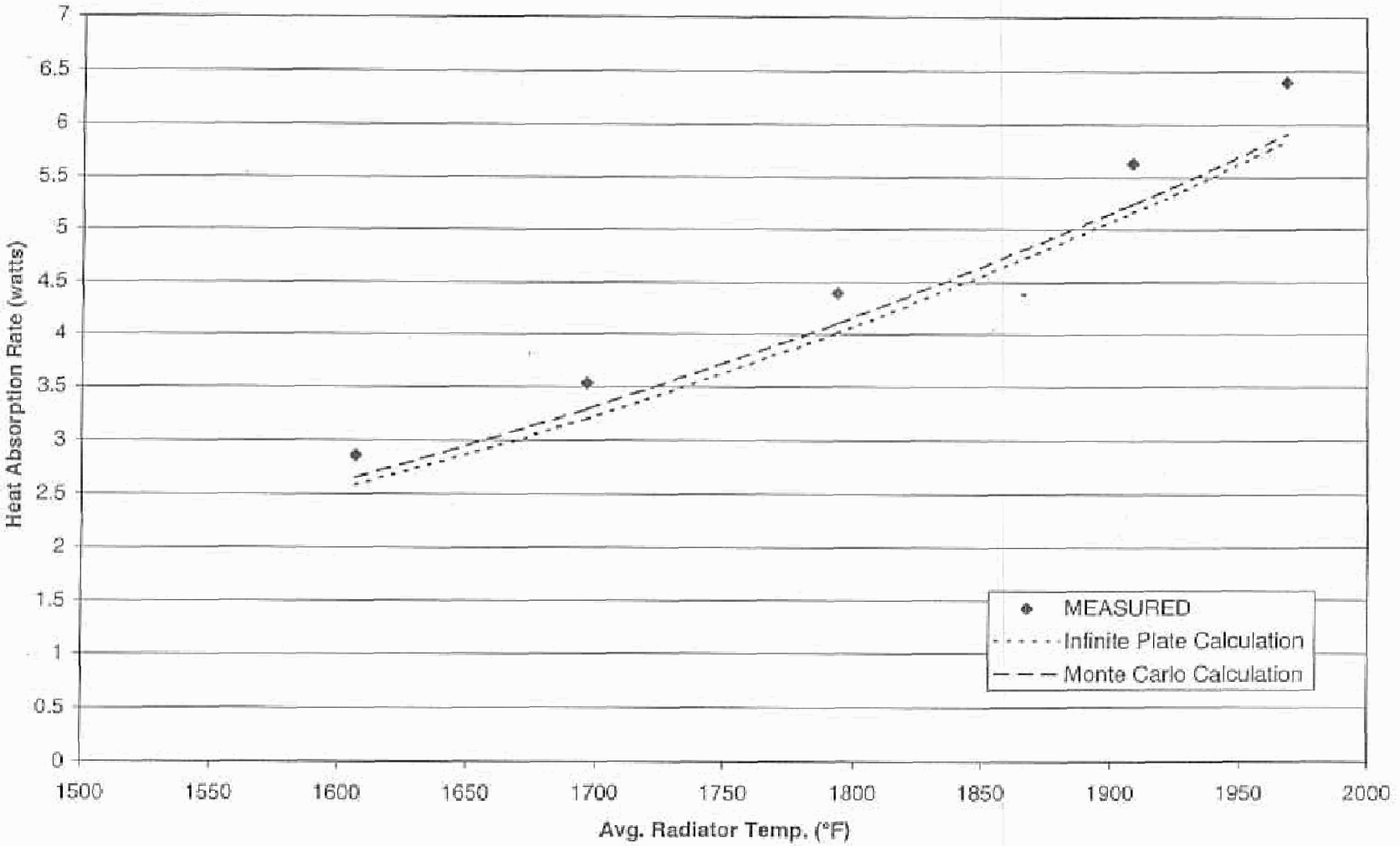

FIGURE 8 - Load Matched (Peak) Power vs. Average Radiator Temperature
TPV Module Tested in Photonic Cavity System

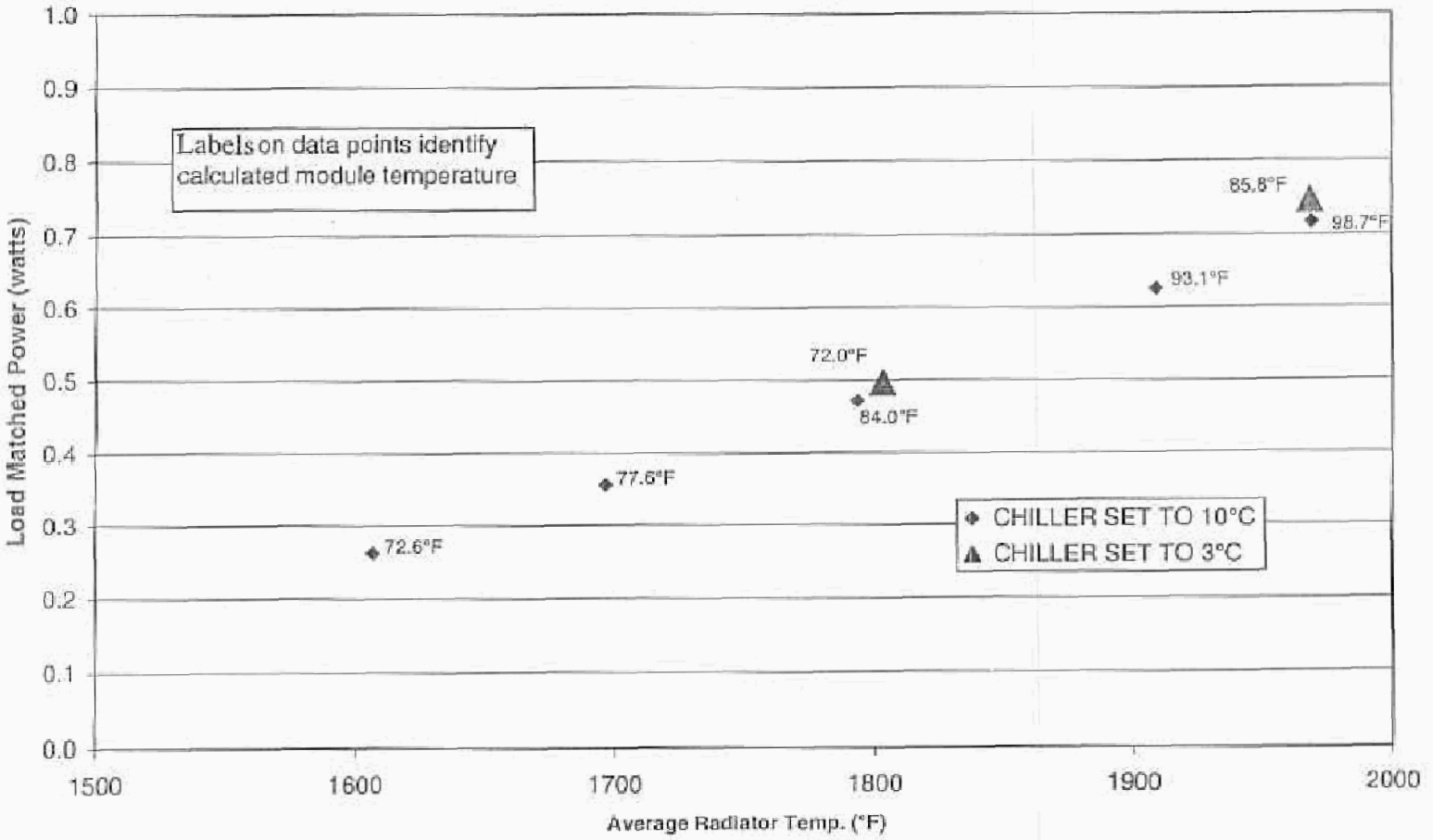

Figure 9 – Calibration Results for the Cavity Test Pedestal together with 95% Confidence Intervals

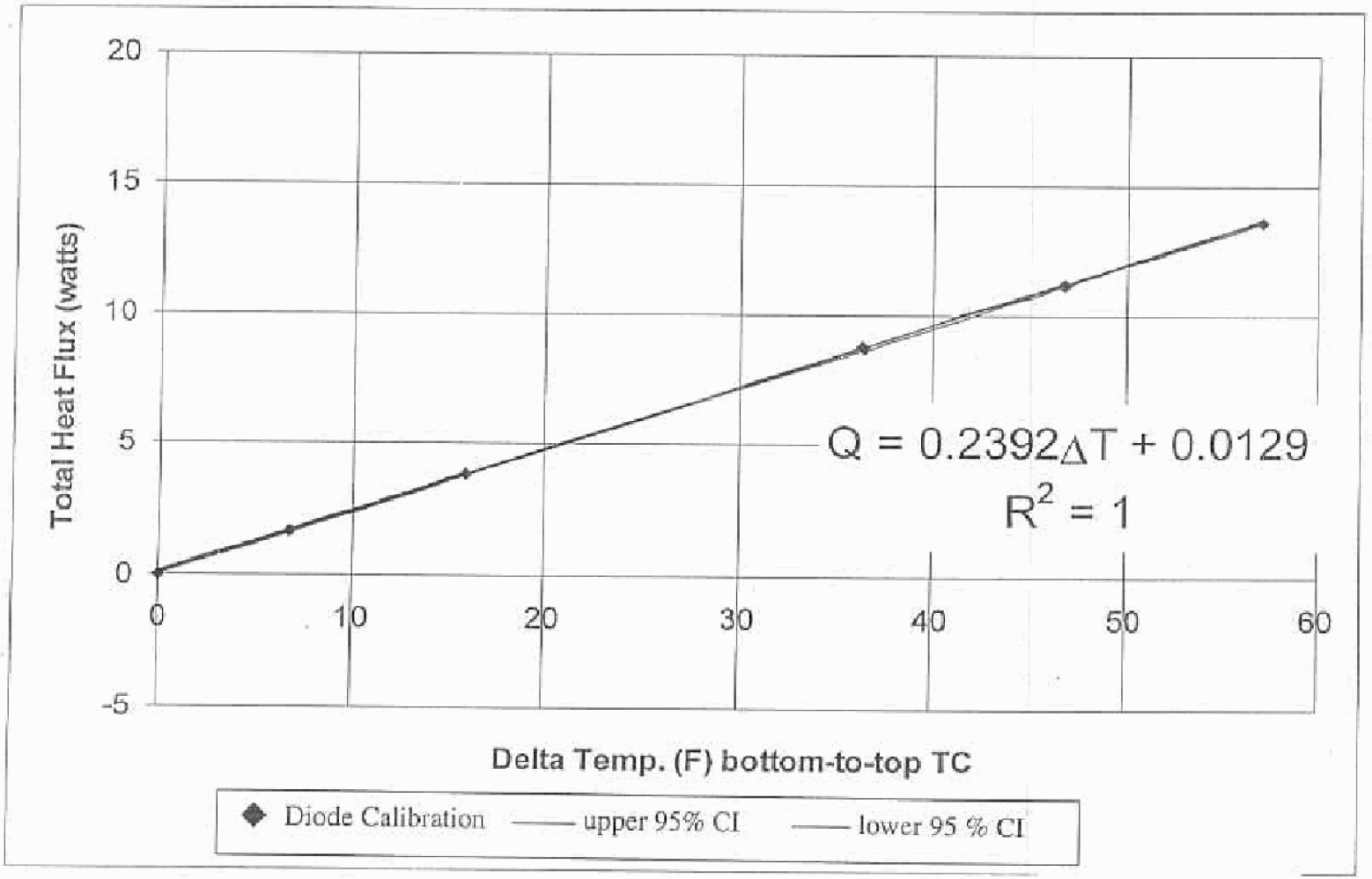

Figure 10 – Module Efficiency as a Function of Average Radiator Temperature Showing 95% Confidence Intervals